**Title**

Unusual aggregates from the oxidation of alkene self-assembled monolayers: a previously unrecognized mechanism for SAM ozonolysis?

**Permalink**

https://escholarship.org/uc/item/5gm6z8pw

**Journal**

Physical chemistry chemical physics : PCCP, 7(20)

**ISSN**

1463-9076

**Authors**

McIntire, Theresa M
Scott Lea, A
Gaspar, Daniel J
et al.

**Publication Date**

2005-10-21

Peer reviewed

# Unusual aggregates from the oxidation of alkene self-assembled monolayers: a previously unrecognized mechanism for SAM ozonolysis?

Theresa M. McIntire,[a] A. Scott Lea,[b] Daniel J. Gaspar,[b] Navdeep Jaitly,[b] Yael Dubowski,[c] Qiguang Li[a] and Barbara J. Finlayson-Pitts*[a]

[a] Department of Chemistry, University of California Irvine, Irvine, CA 92697-2025, USA.
E-mail: bjfinlay@uci.edu; Fax: (949) 824-3168; Tel: (949) 824-7670
[b] Pacific Northwest National Laboratory, Post Office Box 999, MSIN K8-93, Richland, WA 99352, USA
[c] Faculty of Environmental and Civil Engineering, Technion-Israel Institute of Technology, Haifa, 32000, Israel

Self-assembled monolayers (SAMs) of vinyl-terminated 3- and 8-carbon compounds were generated on Si substrates and reacted at room temperature with $\sim 1$ ppm gaseous $O_3$. A combination of atomic force microscopy (AFM), scanning electron microscopy (SEM), Auger electron spectroscopy (AES) and time-of-flight secondary ion mass spectrometry (TOF-SIMS) was used to study the surface composition and morphology after oxidation. A distribution of large ($\sim 0.1$–10 μm) organic aggregates was formed, while the surrounding substrate became depleted of carbon compared to the unreacted SAM. This highly unusual result establishes that the mechanism of ozonolysis of alkene SAMs must have a channel that is unique compared to that in the gas phase or in solution, and may involve polymerization induced by the Criegee intermediate (CI). Oxidation at 60% RH led to the formation of a number of smaller aggregates, suggesting water intercepted the CI in competition with aggregate formation. The uptake of water, measured using transmission FTIR, was not increased upon oxidation of these films. In conjunction with literature reports of polymer formation from VOC-$NO_x$ photooxidations, these results suggest that formation of aggregates and polymers in the atmosphere is much more widespread than previously thought. The implications for the ozonolysis of alkenes on surfaces, for the transformation of organics in the atmosphere, and for the reactions and stability of unsaturated SAMs, are discussed.

## Introduction

Self-assembled monolayers (SAMs) on solids are important for the control of surface properties of materials. They have also been used as model systems, for example for biological membranes[1] and for organics on the surface of airborne dust particles.[2–7] Conversion of these SAMs to other species has been of interest for a number of reasons, including the stability of SAMs in air, the potential for modification of the surface properties through reactions of the SAM, and in applications such as photolithography.[8–12]

Oxidation of alkane SAMs, often in the presence of UV radiation, has been the subject of many studies (e.g., see ref. 8–21). While the vast majority of the work to date has focused on alkanethiol SAMs on gold, several studies of the ozone oxidation of C8 and C3 terminal-alkene SAMs on silica surfaces have been reported.[2–5,7,22] These reactions are faster than expected based on gas phase chemistry, and the products include HCHO, $CO_2$, and CO in the gas phase,[3,5,7,22] and carboxylic acids and perhaps aldehydes on the surface.[3,7] The reaction of ozone with an alkene-terminated thiol SAM on gold under high vacuum has been reported to generate not only the acid, but subsequently the anhydride,[23] which was attributed to reaction of adjacent carboxylic acid groups with elimination of water. Such products appear to be consistent with the well-known mechanisms of oxidation of alkenes by ozone,[24] which proceed via the initial formation of a primary ozonide, followed by its decomposition to an aldehyde and a Criegee intermediate (CI) which can decompose, rearrange to a carboxylic acid, or react with other species such as aldehydes or water. Recent studies of the oxidation of alkenes such as oleic acid particles and/or coated particles suggest that the CI can also react with carboxylic acids and alkenes to form larger compounds.[25–32]

We report here the first observation of large organic aggregates on the surface generated in the ozone oxidation of terminal alkene SAMs. This surprising result shows that there is a previously unrecognized reaction mechanism for the ozonolysis of alkene SAMs, which has potentially important implications for the control of surface properties via oxidation of SAMs, and for the use of ozone as a cleaning agent for such surfaces.[14] In addition, it is relevant to changes in the chemical and physical properties of organics adsorbed on airborne dust particles, which are distributed globally,[33] and which undergo oxidation during transport.

## Experimental

Two different types of substrates were used in these studies. One was p-doped Si(111) wafers (Wacker Siltronic Corp.) and the second consisted of fragments from broken, unused silicon attenuated total reflectance (ATR) elements (Harrick Scientific). For both samples, the substrates were cleaned by boiling sequentially in ethanol and chloroform, and then cleaned in a plasma cleaner on low RF power using Ar for 10 min. The trichlorosilane SAM precursors (7-octenyltrichlorosilane (C8=), 97%, Pfaltz & Bauer; allyltrichlorosilane (C3=), 95%, Sigma-Aldrich Corp.) were dissolved in hexadecane (99%,

Acros Organics) to form a solution that was ~60 mM, and the substrate suspended in this solution for 30 min. The samples were then boiled in chloroform and wiped with laboratory lens paper to remove extraneous polymerized material that was not covalently bound to the surface. Exposure to ozone was carried out by placing the coated SAM sample in a Teflon reaction chamber through which $O_3$, generated using a pen-ray lamp, flowed. The concentration of ozone was determined from the UV absorption at 254 nm and the flow rates of the $O_3/O_2$ from the pen-ray lamp and that of the He diluent gas. The relative humidity was below the detection limit of the RH gauge, which was 5%. In the experiments with added water vapor, a stream of He was passed through a bubbler to generate ~100% RH and this was diluted with dry gas to obtain 60% RH.

Intermittent contact mode AFM images were obtained in air at ambient pressure and humidity using a ThermoMicroscopes AutoProbe CP Research (ThermoMicroscopes, Sunnyvale, CA; now Veeco, Santa Barbara, CA) scanning probe microscope. The piezoelectric scanner was calibrated using a 1.0 μm grating in the x- and y-directions and in the z-direction using several conventional height standards. The tips were V-shaped silicon (Ultrasharp cantilevers, model no. NSC11, Mikro-Masch). Topographs were obtained as 256 × 256 pixels and were flattened line by line and analyzed using AutoProbe image processing software supplied by the manufacturer of the AFM.

Specimens for scanning electron microscopy (SEM) analysis were coated with a thin (~20 nm) layer of gold using a thermal evaporator (Ernest F. Fullam Inc., Latham, NY). The metal thickness was monitored using a Sigma Instruments, Inc. SQM Rate/Thickness Monitor. Metal deposition rate and thickness were measured by the frequency shift of a quartz crystal oscillator over time. SEM images were obtained on gold-coated samples using a Philips FEG-30XL microscope with an accelerating voltage of 10 keV.

The Auger electron spectroscopy (AES)/scanning Auger microprobe was a Physical Electronics Model 680 Auger Nanoprobe based upon a Schottky field emission electron source and a cylindrical mirror analyzer with a multichannel detector. The PHI 680 is equipped with a secondary electron detector to obtain secondary electron images of the uncoated samples during analysis. This instrument provides information about elemental composition of the outer surface (~50–100 Å) of samples at very high magnifications. A 10 nA, 10 kV beam with a size of 26 nm was used to collect Auger electron spectroscopy data. The base system pressure was ~$2 \times 10^{-9}$ Torr. Low resolution survey spectra were taken to identify the elements present in the sample. Multiplex spectra of the identified elements were used in most of the sample quantifications. For quantification, the raw data underwent a nine-point Savitsky–Golay smoothing algorithm followed by a five-point differentiation before applying the pure element sensitivity factors.

TOF-SIMS analysis was carried out using a TRIFT II instrument with a $^{69}Ga^+$ primary beam in both a high mass resolution mode (15 kV, <1 ns pulse width, 600 pA, $m/\Delta m \sim$ 5000), and a high spatial resolution mode (25 kV, ~10 ns pulse width, 60 pA, $m/\Delta m \sim$ 1000). All spectra were taken without charge compensation in the static limit (<$10^{13}$ ions cm$^{-2}$). The summed spectra for an entire image were analyzed to determine contaminant and majority species, and the hyperspectral images were subjected to a principal component analysis (PCA). Prior to the PCA, each mass spectrum in an image was binned to 1 amu, autoscaled and truncated to 200 amu.[34]

## Results and discussion

Fig. 1 shows AFM images of (a) a clean silicon substrate, (b) a Si substrate coated with a SAM of the eight-carbon terminal alkene (C8$^=$), and (c) the sample shown in (b) but after oxidation with ~$10^{13}$ molecules cm$^{-3}$ $O_3$ in the absence of
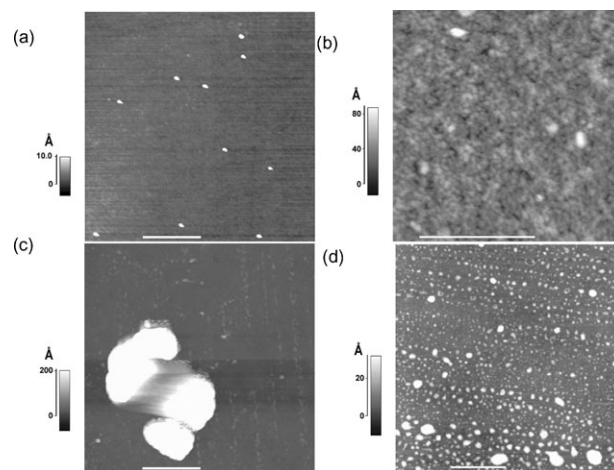


**Fig. 1** Intermittent contact mode AFM images of (a) a clean Si substrate; (b) a Si-substrate on which a C8$^=$ SAM has been deposited; (c) as in (b) but after reaction with ~$10^{13}$ molecules cm$^{-3}$ $O_3$ for 40 min; (d) a C8$^=$ SAM after ozone oxidation in presence of water at 60% RH. The scale bar in all images is 500 nm.

water vapor (RH <5%). Small particles are observed on the clean substrate which Auger scanning microprobe spectroscopy (see below) indicates are typically small particles of silica, likely caused by "chipping" of the surface during handling. The organic-coated sample in (b) shows a relatively smooth surface as expected for a SAM on Si. However, after oxidation with $O_3$, large, irregular particles are observed. The particle sizes, shapes and distribution on the substrate are quite heterogeneous, with the dimensions varying from tens of nanometres to the upper limit of the AFM of several micrometres. Similar observations were made for Si coated with a C3$^=$ SAM. As a check, long-chain C8 and C12 saturated SAMs were generated on a silicon substrate and exposed to $O_3$ under similar conditions. AFM, ATR-FTIR and TOF-SIMS studies showed no evidence for reaction of these saturated SAMs on exposure to $O_3$.

SEM was applied to unreacted and ozone-oxidized samples of the C8$^=$ SAM that had been gold-coated to preserve their morphology in order to search for larger features that could not be probed using AFM. The unoxidized sample showed no significant morphological features, consistent with the AFM results. However, the oxidized sample showed not only micrometre-sized aggregates, but also features as large as ~10 μm (Fig. 2), which appeared very irregular and porous in nature. SEM and AFM are optimized for different length scales so that the smallest features seen by AFM are not observable in these images. The wide distribution of particle sizes, shapes and number density may be due to reaction being initiated at defects and/or steps and edges in the SAM.[9]

Scanning Auger microprobe analysis was used to probe the elemental composition of particles such as that in Fig. 3a from the reaction of the C3$^=$ SAM with $O_3$. Fig. 3b shows the elemental composition along the line in the SEM of Fig. 3a. As expected if the features are organic, the C and O signals increase across the balls and the Si decreases due to shielding of the substrate. Quantification is complicated by beam damage during analysis, by contributions from adventitious carbon and by the possibility of increased oxygen on the substrate after the exposure to ozone. With those caveats, analysis on and off a number of particles obtained by extrapolating back to a beam dose of zero showed that reaction decreased the C/Si ratio on areas surrounding the particles to $0.6 \pm 0.1$ of that for the unreacted SAM in the case of C3$^=$, and to $0.8 \pm 0.1$ for C8$^=$. This is supported by preliminary TOF-SIMS data subjected to principal component analysis which show that the substrate after oxidation of C8$^=$ consists largely
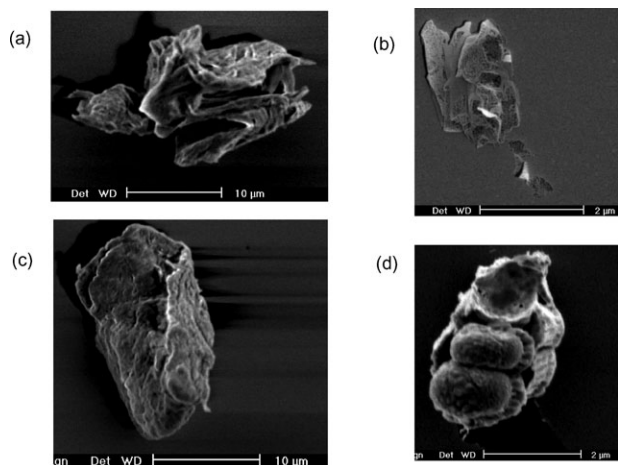
**Fig. 2** Some typical SEM images of a C8$^=$ SAM after reaction with $\sim 10^{13}$ molecule cm$^{-3}$ O$_3$ for 40 min.

of Si and Si-containing clusters (SiOH, SiO$_2$H *etc.*), indicating that much (but not necessarily all) of the SAM has been removed. As expected based on Fig. 3a, on the particles themselves the C/Si ratio increased by a factor of $1.7 \pm 1.4$ for C3$^=$, and $1.3 \pm 1.1$ for C8$^=$, compared to the unreacted SAM.

All of these data taken together show that ozone oxidation of the vinyl-terminated SAMs leads to agglomeration of organic in the original SAM into the large features observed by AFM, SEM, and AES. While this observation is very surprising, particularly for a system where only a monolayer of material is available, a simple calculation shows that there is sufficient reactant available to form these features. There is such a wide variation in particle sizes, shapes and number densities from one region of the sample to another that an accurate estimate of the total volume of particles formed on the sample is precluded. In addition, while the images show that the particles are porous, their density is not known. However, take the extreme case of the largest ($\sim 10$ μm) particles, which are typically found after scanning half a dozen areas approximately 200 μm $\times$ 200 μm in size. In such an area, the total number of SAM molecules is $7.4 \times 10^{11}$ based on a SAM surface density[7] of $3.1 \times 10^{14}$ SAM cm$^{-2}$, and these have a mass of $1.4 \times 10^{-10}$ g based on the CH$_2$=CH(CH$_2$)$_6$ portion of the SAM. The AFM studies of the smaller particles indicate the height of the particles is typically $\sim 20\%$ of their width and
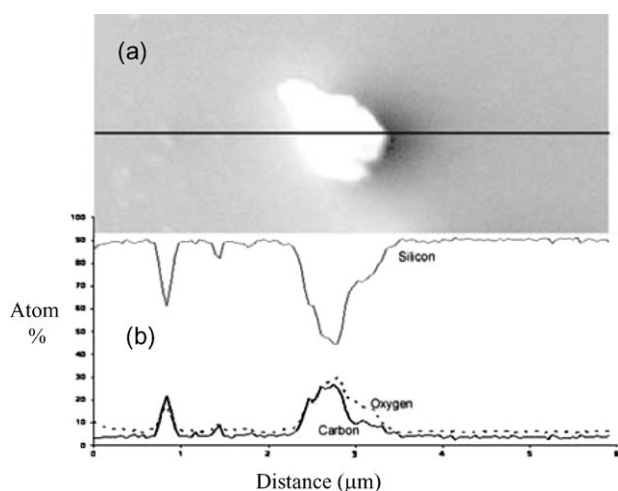
length. A particle of dimensions 10 μm $\times$ 10 μm $\times$ 2 μm has a volume of $2 \times 10^{-10}$ cm$^3$. A particle of this size that incorporated all of the SAM from the 6 $\times$ 200 μm $\times$ 200 μm area would therefore have a density of 0.7 g cm$^{-3}$. This is a reasonable upper limit, given the porous nature of the particles (Fig. 2) and that there is likely residual carbon from the SAM remaining on the substrate.

It is likely that these large features are organic polymers, although attempts at mass spectral analysis of the particles directly on the substrate or after removal by sonication have not been successful to date. Nucleation and growth of small organic oxidation products into aggregates cannot be ruled out, although it would be surprising that such a mechanism would lead to the irregular, seemingly porous material (Fig. 2) rather than a more spherical "droplet" on the surface. In any event, these data clearly establish that a previously unrecognized mechanism contributes significantly to the oxidation of alkene SAMs on silica surfaces.

Ozone–alkene reactions are known to occur in the gas phase and in solution by the initial formation of a primary ozonide that decomposes to an aldehyde or ketone and a Criegee intermediate (Fig. 4). There are a number of well-known reaction paths for the CI, including reaction with an aldehyde to generate a secondary ozonide or decomposition to generate OH free radicals[24] which could initiate polymerization. In previous studies,[7] adding ethane to the gas phase as an OH trap had no impact on the formation of surface products; however, if OH were formed inside the SAM, it might not escape to the gas phase. Other possibilities include the reaction of the CI with adjacent unreacted alkenes or with carboxylic acids formed in the initial reaction, both which have been proposed based on product yields in the reaction of ozone with oleic acid particles.[25–32] Ziemann and coworkers have shown that hydroperoxides react with aldehydes to form peroxyhemiacetals which can react further with carboxylic acids to form larger peroxides.[28–30,32] If hydroperoxides were key intermediates in the SAM oxidation, the addition of water should increase their formation and hence that of the aggregates. As seen in Fig. 1d, the presence of water has the opposite effect. This is consistent with a competition between reactions of the CI that lead to polymer formation, and that with water vapor.

In previous studies in this laboratory,[7] the kinetics showed Langmuir-Hinshelwood behaviour, with an experimentally derived residence time for adsorbed ozone of about 7 s, much greater than $\sim 15$ ps calculated for van der Waals interactions of ozone with a SAM surface. The present results suggest that the discrepancy may be due to ozone adsorbing to the silica substrate, which is initially available as small holes in the SAM (Fig. 1b) and which becomes increasing exposed as the organic is swept up into the large features on the surface. Alternatively, or perhaps in addition, ozone may dissolve in the aggregates themselves so that they act as a reservoir for ozone on the surface. Ozone is more soluble in organics than in water; for example, the Henry's law constant[35,36] for ozone in oleic acid is $\sim 0.1$ M atm$^{-1}$, about an order of magnitude larger than the value for dissolution in water.[24]

Airborne particles have well-documented effects on human health, visibility and the chemistry and radiative properties of the atmosphere.[24,37,38] Dust storms provide large, episodic sources of particles that can be distributed globally.[33,39,40] Mineral dust, of which silica is commonly a major component,[5,24] adsorbs organic compounds which are oxidized during transport.[41,42] Oxidation is thought to convert hydrophobic coatings into polar, hydrophilic coatings that will adsorb increased amounts of water (*e.g.,* see refs. 2, 43 and 44) influencing the chemical and radiative properties of the particles. However, the present studies show that as oxidation proceeds, the underlying substrate is increasingly exposed. This suggests that the model of conversion of fully coated organic hydrophobic particles into a uniform, hydrophilic coating that
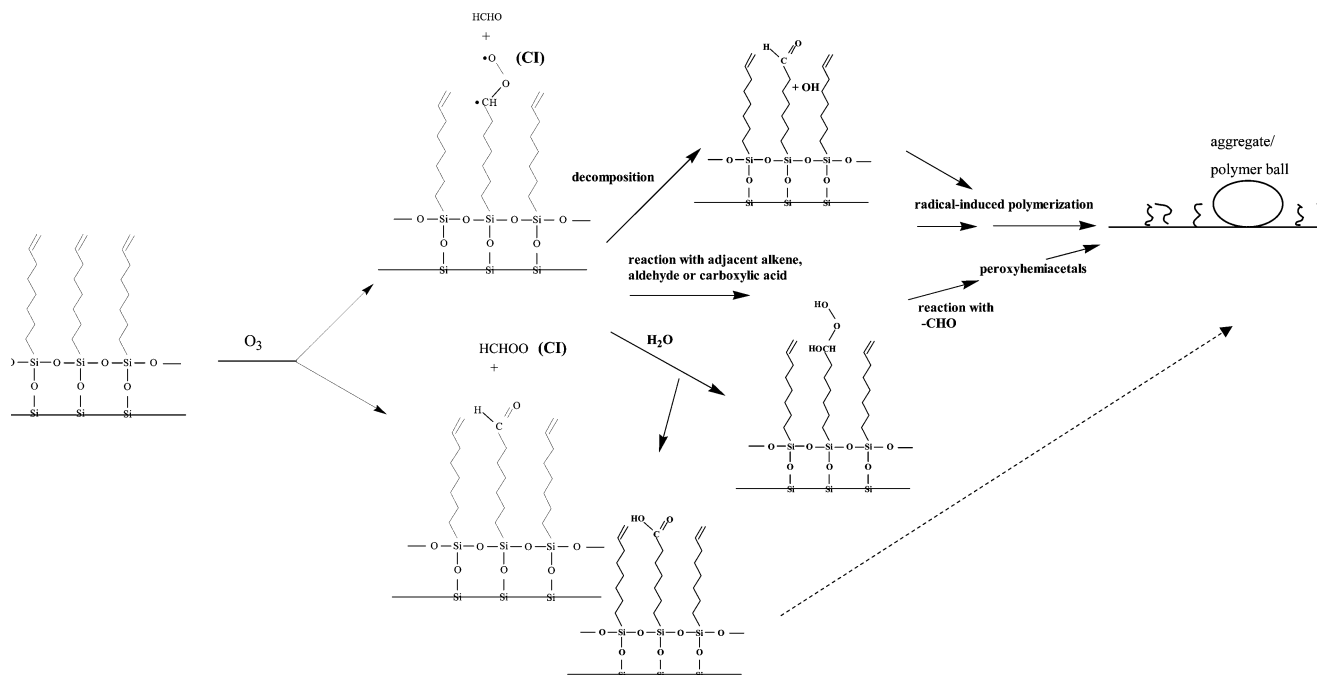


**Fig. 3** (a) Auger image of C3$^=$ particles after reaction with $\sim 10^{13}$ molecules cm$^{-3}$ O$_3$ for 40 min; (b) line scan of particles showing they are composed of carbon and oxygen. These data should be taken as semi-quantitative, since they have not been corrected for beam damage which has the greatest impact on oxygen, particularly on the substrate.

**Fig. 4** Overall scheme for ozone oxidation of unsaturated SAMs on a silica surface. For simplicity, the excited and stabilized Criegee intermediates (CI) have not been shown separately.

takes up increased amounts of water may not, indeed, be the case.

Fig. 5 shows the amount of surface-adsorbed water at equilibrium at various relative humidities (RH) measured using methods described elsewhere[45] for an unreacted C8$^=$ SAM, an ozone-oxidized C8$^=$ SAM and, for comparison, an unreacted saturated C18 SAM, all on quartz substrates. The water adsorbed on the less-ordered, unreacted C8$^=$ SAM (which is within experimental error of that on a clean quartz substrate) is larger than on the well-ordered, relatively defect-free C18 SAM. This is consistent with defects and imperfections on the C8$^=$ SAM through which water can penetrate to the substrate.[46–48] However, there is no difference in water uptake before and after the oxidation of the C8$^=$ SAM. The C3$^=$ SAM showed similar behavior. Donaldson and coworkers[49] reported increased water uptake upon oxidation of oleic acid on quartz, and based on infrared spectroscopic measurements, proposed that polymerization had occurred. However, their films were prepared by spreading oleic acid on the surface using a cotton swab and were there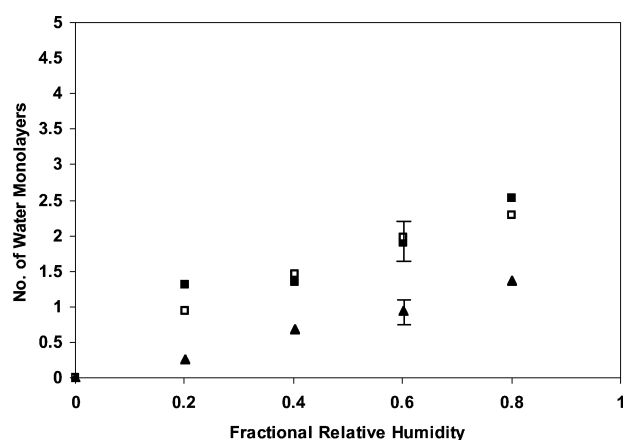fore more likely similar to the bulk material rather than a monolayer as was the case in the present studies. In addition, very high (hundreds of ppm) concentrations of ozone were used, and it has been shown for oleic acid particles[50] that water uptake increases with ozone exposure. For SAM monolayers and lower concentrations of ozone, oxidation of the SAM clearly does not lead to enhanced water uptake, which may be due to control of water uptake by the substrate for both the reactant and for the oxidized sample.

Ozone, a toxic air pollutant for which air quality standards are set, is found in the atmosphere globally at $\sim$30–40 ppb in remote regions, and higher levels in polluted areas.[24] It is also generated by some indoor "air purifiers".[51] The results presented here suggest that alkene SAMs may not have long-term stability in ambient air that contains even "background" amounts of ozone and that the formation of these large organic aggregates may occur more generally when alkenes are present on a surface, e.g., from materials or household cleaning products. In addition, this oxidation leads to surface segregation of the organic material, which will change the interactions of the particle with biological systems, e.g., the surface of the lung upon inhalation, in ways that remain to be explored.

In studies of the atmospheric oxidation of organic compounds, less than 50% of the condensed phase products in particles have typically been identified.[24,52] Recent laboratory studies[53–59] indicate that the missing material is at least in part polymeric. Whether the reactions leading to the polymers require acid-catalysis is not clear. However, the present studies show that the formation of organic aggregates and/or polymeric material in airborne particles may be a quite general phenomenon that is not restricted to reactions of secondary organics in the liquid phase, nor to acid-catalyzed chemistry.

Finally, ozone, often in combination with UV radiation, is frequently used for "cleaning" organics from surfaces. It has been reported[14] that this treatment leaves some residual carbon on the surface. It may be that this residual carbon is aggregated organic material similar to that observed in these studies. Once the double bond has been reacted, such material would be relatively impervious to treatment by ozone alone. These large features would also be far less reactive towards species such as O($^3$P), O($^1$D) and OH generated by photolysis than would a monolayer of material, since oxidation would have to occur layer-by-layer.



**Fig. 5** Water uptake as a function of RH at 295 K measured using FTIR as described in detail elsewhere (32). C18 SAM (▲); C8$^=$ SAM (■); and C8$^=$ after reaction with $\sim$10$^{13}$ molecules cm$^{-3}$ O$_3$ for 40 min (□). Representative error bars are given for the C18 and oxidized C8$^=$ SAMs.

Studies are underway to identify the composition of the particles and to investigate their dependence on the structure of the parent SAM, reaction time and concentrations of ozone and water vapor. This will elucidate the detailed mechanism of the ozonolysis of alkene SAMs, which is needed for controlling their surface properties and for understanding the oxidation of unsaturated organics on surfaces, including SAMs, under a variety of conditions in air.

## Acknowledgements

## References

1 S. Lingler, I. Rubinstein, W. Knoll and A. Offenhausser, *Langmuir*, 1997, **13**, 7085.
2 T. Moise and Y. Rudich, *J. Geophys. Res.*, 2000, **105**, 14667.
3 E. R. Thomas, G. J. Frost and Y. Rudich, *J. Geophys. Res.*, 2001, **106**, 3045.
4 Y. Rudich, *Chem. Rev.*, 2003, **103**, 5097.
5 C. R. Usher, A. E. Michel and V. H. Grassian, *Chem. Rev.*, 2003, **103**, 4883.
6 M. Molina, A. V. Ivanov, S. Trakhtenberg and L. T. Molina, *Geophys. Res. Lett.*, 2004, **31**, DOI: 10.1029/2004GL020910.
7 Y. Dubowski, J. Vieceli, D. J. Tobias, A. Gomez, A. Lin, S. A. Nizkorodov, T. M. McIntire and B. J. Finlayson-Pitts, *J. Phys. Chem. A*, 2004, **108**, 10473.
8 M. H. Schoenfisch and J. E. Pemberton, *J. Am. Chem. Soc.*, 1998, **120**, 4502.
9 G. E. Poirier, T. M. Herne, C. C. Miller and M. J. Tarlov, *J. Am. Chem. Soc.*, 1999, **121**, 9703.
10 M. M. Ferris and K. L. Rowlen, *Appl. Spectrosc.*, 2000, **54**, 664.
11 J. Y. Huang, D. A. Dahlgren and J. C. Hemminger, *Langmuir*, 1994, **10**, 626.
12 J. M. Behm, K. R. Lykke, M. J. Pellin and J. C. Hemminger, *Langmuir*, 1996, **12**, 2121.
13 T. Ye, D. Wynn, R. Dudek and E. Borguet, *Langmuir*, 2001, **17**, 4497.
14 D. W. Moon, A. Kurokawa, S. Ichimura, H. W. Lee and I. C. Jeon, *J. Vac. Sci. Technol. A*, 1999, **17**, 150.
15 Y. Paz, S. Trakhtenberg and R. Naaman, *J. Phys. Chem.*, 1992, **96**, 10964.
16 Y. Paz, S. Trakhtenberg and R. Naaman, *J. Phys. Chem.*, 1993, **97**, 9075.
17 Y. Paz, S. Trakhtenberg and R. Naaman, *J. Phys. Chem.*, 1994, **98**, 13517.
18 M. Lewis, M. Tarlov and K. Carron, *J. Am. Chem. Soc.*, 1995, **117**, 9574.
19 J. Y. Huang and J. C. Hemminger, *J. Am. Chem. Soc.*, 1993, **115**, 3342.
20 E. A. McArthur, T. Ye, J. P. Cross, A. Petoud and E. Borguet, *J. Am. Chem. Soc.*, 2004, **126**, 2260.
21 K. Uosaki, M. E. Quayum, S. Nihonyanagi and T. Kondo, *Langmuir*, 2004, **20**, 1207.
22 C. R. Usher, A. E. Michel, D. Stec and V. H. Grassian, *Atmos. Environ.*, 2003, **37**, 5337.
23 L. R. Fiegland, M. M. S. Fleur and J. R. Morris, *Langmuir*, 2005, **21**, 2660.
24 B. J. Finlayson-Pitts and J. N. Pitts Jr., *Chemistry of the Upper and Lower Atmosphere-Theory, Experiments, and Applications*, Academic Press, San Diego, CA, 2000.
25 Y. Katrib, S. T. Martin, H.-M. Hung, Y. Rudich, H. Zhang, J. G. Slowick, P. Davidovits, J. T. Jayne and D. R. Worsnop, *J. Phys. Chem. A*, 2004, **108**, 6686.
26 J. D. Hearn and G. D. Smith, *J. Phys. Chem A*, 2004, **108**, 10019.
27 J. D. Hearn, A. J. Lovett and G. D. Smith, *Phys. Chem. Chem. Phys.*, 2005, **7**, 501.
28 H. J. Tobias, K. S. Docherty, D. E. Beving and P. J. Ziemann, *Environ. Sci. Technol.*, 2000, **34**, 2116.
29 H. J. Tobias and P. J. Ziemann, *Environ. Sci. Technol.*, 2000, **34**, 2105.
30 K. S. Docherty, W. Wu, Y. B. Lim and P. J. Ziemann, *Environ. Sci. Technol.*, 2005, **39**, 4049.
31 P. J. Ziemann, *J. Phys. Chem. A*, 2003, **107**, 2048.
32 P. J. Ziemann, *Faraday Discuss.*, 2005, **130**, 469.
33 J. M. Prospero and R. T. Nees, *Science*, 1977, **196**, 1196.
34 M. S. Wagner, D. J. Graham, B. D. Ratner and D. G. Castner, *Surf. Sci.*, 2004, **570**, 78.
35 T. Moise and Y. Rudich, *J. Phys. Chem. A*, 2002, **106**, 6469.
36 J. W. Morris, P. Davidovits, J. T. Jayne, J. L. Jimenez, Q. Shi, C. E. Kolb, D. R. Worsnop, W. S. Barney and G. Cass, *Geophys. Res. Lett.*, 2002, **29**, DOI: 10.1029/2002GL014692.
37 C. A. I. Pope, R. T. Burnett, M. J. Thun, E. E. Calle, D. Krewski, K. Ito and G. D. Thurston, *J. Am. Med. Assoc.*, 2002, **287**, 1132.
38 Intergovernmental Panel on Climate Change, *Change Climate 2001: The Scientific Basis*, ed. J. T. Houghton, Y. Ding, D. J. Griggs, M. Noguer, P. J. v. d. Linden, X. Dai, K. Maskell and C. A. Johnson, Cambridge University Press, Cambridge, 2001.
39 L. J. DeBell, M. Vozzella, R. W. Talbot and J. E. Dibb, *J. Geophys. Res.*, 2004, **109**, DOI: 10.1029/2003JD003733.
40 Y. Gu, W. I. Rose and G. J. S. Bluth, *Geophys. Res. Lett.*, 2003, **30**, DOI: 10.1029/2003GL017405.
41 A. H. Falkovich, G. Schkolnik, E. Ganor and Y. Rudich, *J. Geophys. Res.*, 2004, **109**, DOI: 10.1029/2003JD003919.
42 L. M. Russell, S. F. Maria and S. C. B. Myneni, *Geophys. Res. Lett.*, 2002, **29**, DOI: 10.1029/2002GL014874.
43 A. K. Bertram, A. V. Ivanov, M. Hunter, L. T. Molina and M. J. Molina, *J. Phys. Chem. A*, 2001, **105**, 9415.
44 Y. Katrib, S. T. Martin, Y. Rudich, P. Davidovits, J. T. Jayne and D. R. Worsnop, *Atmos. Chem. Phys.*, 2004, **4**, 6431.
45 A. L. Sumner, E. J. Menke, Y. Dubowski, J. T. Newberg, R. M. Penner, J. C. Hemminger, L. M. Wingen, T. Brauers and B. J. Finlayson-Pitts, *Phys. Chem. Chem. Phys.*, 2004, **6**, 604.
46 I. Diez-Pérez, M. Luna, F. Teherán, D. F. Ogletree, F. Sanz and M. Salmeron, *Langmuir*, 2004, **20**, 1284.
47 E. Thomas, S. Trakhtenberg, R. Ussyshkin and Y. Rudich, *J. Geophys. Res.*, 1999, **104**, 16053.
48 M. Wang, K. M. Liechti, Q. Wang and J. M. White, *Langmuir*, 2005, **21**, 1848.
49 A. Asad, B. T. Mmereki and D. J. Donaldson, *Atmos. Chem. Phys.*, 2004, **4**, 2083.
50 K. E. Broekhuizen, T. Thornberry, P. P. Kumar and J. P. D. Abbatt, *J. Geophys. Res.*, 2004, **109**, DOI: 10.1029/2004JD005298.
51 N. Britigan, A. Alshawa and S. Nizkorodov, 2005, submitted for publication.
52 M. S. Jang, N. M. Czoschke, S. Lee and R. M. Kamens, *Science*, 2002, **298**, 814.
53 M. Kalberer, D. Paulsen, M. Sax, M. Steinbacher, J. Dommen, A. S. H. Prevot, R. Fisseha, E. Weingartner, V. Frankevich, R. Zenobi and U. Baltensperger, *Science*, 2004, **303**, 1659.
54 M. P. Tolocka, M. Jang, J. M. Ginter, F. J. Cox, R. M. Kamens and M. V. Johnston, *Environ. Sci. Technol.*, 2004, **38**, 1428.
55 S. Gao, M. Keywood, N. L. Ng, J. Surratt, V. Varutbangkul, R. Bahreini, R. C. Flagan and J. H. Seinfeld, *J. Phys. Chem. A*, 2004, **108**, 10147.
56 S. Gao, N. L. Ng, V. Varutbangkul, R. Bahreini, A. Nenes, J. He, K. Y. Yoo, J. L. Beauchamp, R. P. Hodyss, R. C. Flagan and J. H. Seinfeld, *Environ. Sci. Technol.*, 2004, **38**, 6582.
57 Y. Iinuma, O. Boge, T. Gnauk and H. Herrmann, *Atmos. Environ.*, 2004, **38**, 761.
58 M. Jang, B. Carroll, B. Chandramouli and R. M. Kamens, *Environ. Sci. Technol.*, 2003, **37**, 3828.
59 M. Jang, S. Lee and R. M. Kamens, *Atmos. Environ.*, 2003, **37**, 2125.